Global Journal of Researches in Engineering: E
Civil And Structural Engineering
Volume 17 Issue 1 Version 1.0 Year 2017
Type: Double Blind Peer Reviewed International Research Journal
Publisher: Global Journals Inc. (USA)
Online ISSN: 2249-4596 & Print ISSN: 0975-5861

CFRP Retrofitting Schemes for Prestressed Concrete Box Beams for Highway Bridges

By Herish A. Hussein & Zia Razzaq
Old Dominion University

Abstract- This paper investigates various retrofitting schemes for a prestressed concrete box beam using carbon fiber reinforced polymer (CFRP) sheets with the goal of increasing flexural strength. A simply-supported box beam is studied with a constant uniformly distributed load and three gradually increasing concentrated loads proportional to HS20 truck loading of the Association of State Highway and Transportation Officials (AASHTO). Various retrofitting schemes are considered each with single, double, and triple CFRP sheets, respectively, installed in high compression and tension regions. Cross-sectional nonlinear moment-curvature relations are developed and coupled with a finite-difference solution algorithm to predict load-deflection relations for both retrofitted and non-retrofitted box beams. The study identifies effective CFRP retrofitting schemes that result in a significant increase in the flexural strength of the prestressed concrete box beam.

Keywords: *CFRP retrofitting, highway bridges, box beam, prestressed.*

GJRE-E Classification: *FOR Code: 879999p*

Strictly as per the compliance and regulations of:

CFRP Retrofitting Schemes for Prestressed Concrete Box Beams for Highway Bridges

Herish A. Hussein [α] & Zia Razzaq [σ]

Abstract- This paper investigates various retrofitting schemes for a prestressed concrete box beam using carbon fiber reinforced polymer (CFRP) sheets with the goal of increasing flexural strength. A simply-supported box beam is studied with a constant uniformly distributed load and three gradually increasing concentrated loads proportional to HS20 truck loading of the Association of State Highway and Transportation Officials (AASHTO). Various retrofitting schemes are considered each with single, double, and triple CFRP sheets, respectively, installed in high compression and tension regions. Cross-sectional nonlinear moment-curvature relations are developed and coupled with a finite-difference solution algorithm to predict load-deflection relations for both retrofitted and non-retrofitted box beams. The study identifies effective CFRP retrofitting schemes that result in a significant increase in the flexural strength of the prestressed concrete box beam.

Keywords: CFRP retrofitting, highway bridges, box beam, prestressed.

I. Introduction

Retrofitting prestressed concrete beams to increase their strength is an evolving area of structural engineering research. Retrofitting with carbon fiber reinforced polymer (CFRP) strips or plates has been used in tensile regions of concrete beams [1-3]. CFRP retrofitting material is more advantageous than steel since it is non-corrosive, light-weight, easy to ship, available in practically any length, and easy to install [4-6]. It also exhibits superior fatigue resistance, low thermal expansion, and low relaxation [7-9]. Using CFRP laminar sheets on various parts of beams with high-strength adhesive epoxy can increase flexural strength and even support any damaged strands without having to demolish the affected areas [10-12]. Retrofitting tension regions in beams is of benefit not only to increase strength but also off-set weakness of concrete in tension, and protect prestressing strands from corrosion and vehicle impacts. This paper investigates the effectiveness of using CFRP retrofitting of prestressed concrete box beams in high tensile, compressive, and both tensile and compressive regions. Such retrofitting schemes can provide added strength for highway bridge girders.

Author α: Research Assistant, Ph.D. Candidate, Department of Civil and Environmental Engineering, Old Dominion University, 115 Kaufman Hall, Norfolk, Virginia, USA. e-mail: hhuss001@odu.edu

Author σ: University Professor, Department of Civil and Environmental Engineering, Old Dominion University, 135 Kaufman Hall, Norfolk, Virginia, USA. e-mail: zrazzaq@odu.edu

II. Problem Description

Figure 1 shows a simply-supported prestressed concrete box beam used in highway bridges. The beam is subjected to AASHTO-type of loading in addition to the beam self-weight of 0.842 kips/ft. the external loading consists of a uniformly distributed load of 0.64 kips/ft., and concentrated loads 4P, 4P, and P as shown in Figure 1. The AASHTO loading is obtained if P=8 kips, however, in the present study, the value of P is gradually increased up to collapse condition in the presence of constant uniformly distributed loading. The Type BIII-48 box beam section has two rows of 7-wire ASTM Grade 270 ½ in. diameter strands as shown in Figure 2.

To demonstrate the effectiveness of CFRP retrofitting, an AASHTO Type BIII-48 box beam cross section [13] is adopted in the present study. Figure 2a shows the box beam cross section without retrofitting and is used as a reference beam section to determine the effectiveness of various retrofitting schemes. As shown in this figure, the prestressing is achieved with two rows of strands with 23 strands per row. Figures 2b and 2c show the box beam section retrofitted with a single 40 x 1/16 in. CFRP sheet, in tension and compression regions, respectively. Figure 2d shows the box beam with single CFRP sheets in both tension and compression regions. Figures 2e -2g show similar retrofitting schemes with double CFRP sheets while Figures 2h-2j show those with triple CFRP sheets.

In this study, the following nonlinear normal compressive stress-strain relation for concrete given by Lin and Burns [14] has been adopted:

$$f_c = f_c^{'} \left[2(\epsilon_c / \epsilon_\circ) - (\epsilon_c / \epsilon_\circ)^2\right] \quad (1)$$

where ϵ_c is the concrete strain, and $\epsilon_\circ$ is the concrete strain at ultimate compression strength, $f_c^{'}$. The numerical results presented in this paper are based on a $f_c^{'}$ value of 5.8 ksi and a concrete modulus of elasticity of 4,383 ksi. Each CFRP sheet used for retrofitting has a thickness of 1/16 in. and a width of 40 in. The Young's modulus of CFRP material is 22,000 ksi and it has an ultimate strength of 260 ksi.

The problem addressed in this study is to determine the effectiveness of various retrofitting schemes shown in Figures 2b through 2j with the objective of maximizing the load-carrying capacity of the prestressed concrete box beam shown in Figure 1. This

is achieved by first formulating the nonlinear moment-curvature relations for the ten cross sections shown in Figure 2 followed by theoretical prediction of the load P versus maximum vertical deflection of the beam.

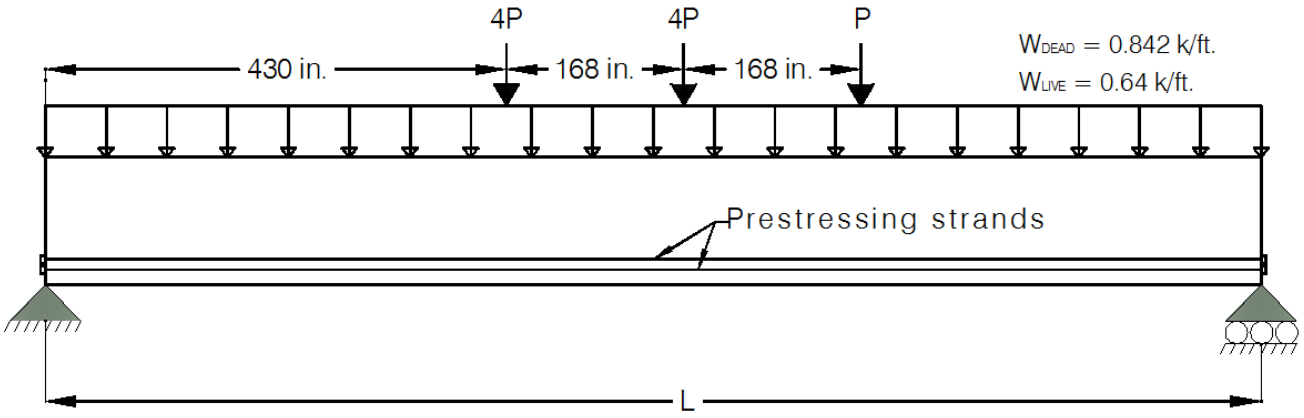

Figure 1: Prestressed concrete box beam with AASHTO-type loading

III. Nonlinear Moment-Curvature Relations

All moment-curvature relations presented in this paper are derived using 7-wire strands prestressed to a force F equal to 160 kips. In the analysis presented, the effects of keys and fillets on the moment-curvature relations for the cross sections in Figure 2 are considered negligible. This approximation results in only a 0.06% difference in the cross-sectional areas. Figure 3 shows the strain and stress distribution for a simply-supported box beam with CFRP retrofitting at the bottom. In this figure, C_c, T_{ps}, and T_{CFRP} are the resultant concrete force, strand force, and CFRP force, respectively. The concrete force is found using:

$$C_c = \int_0^c f_c \times dA = C_{c2} - C_{c1} \quad (2)$$

where:

$C_{c1} = \int_0^{c1} f_c \times b_1 \times dx$

$C_{c2} = \int_0^{c2} f_c \times b_2 \times dx$

dA = elemental concrete area in compression,

b_1, b_2 = inner and outer cross-sectional widths, and

c_1, c_2 = distances from NA shown in Figure 3b.

As seen in Figure 3c, the concrete strain, ϵ_c, can be expressed in terms of the curvature ϕ and distance x from neutral axis (NA):

$$\epsilon_c = \phi \times x \quad (3)$$

Substituting Equations 1 and 3 into Equation 2 results in [14]:

$$C_c = b_2 \times f_c' \times \int_0^{c2} [\frac{2 \times \phi \times x}{\epsilon_o} - (\frac{\phi \times x}{\epsilon_o})^2] \, dx - b_1 \times f_c' \times \int_0^{c1} [\frac{2 \times \phi \times x}{\epsilon_o} - (\frac{\phi \times x}{\epsilon_o})^2] \, dx \quad (4)$$

which upon integration gives:

$$C_c = b_2 \times c_2^2 \times f_c' \times \frac{\phi}{\epsilon_o} (1 - \frac{\phi \times c_2}{3\epsilon_o}) - b_1 \times c_1^2 \times f_c' \times \frac{\phi}{\epsilon_o} (1 - \frac{\phi \times c_1}{3\epsilon_o}) \quad (5)$$

In Figure 2d, X represents the distance of C_c from the NA, and is found using:

$$X \times C_c = \int_0^{c2} f_c \times b_2 \times x \, dx - \int_0^{c1} f_c \times b_1 \times x \, dx \quad (6)$$

Using Equations 1, 5, and 6 gives:

$$X = c_2 (\frac{8\epsilon_o - 3\phi \times c_2}{12\epsilon_o - 4\phi \times c_2}) - c_1 (\frac{8\epsilon_o - 3\phi \times c_1}{12\epsilon_o - 4\phi \times c_1}) \quad (7)$$

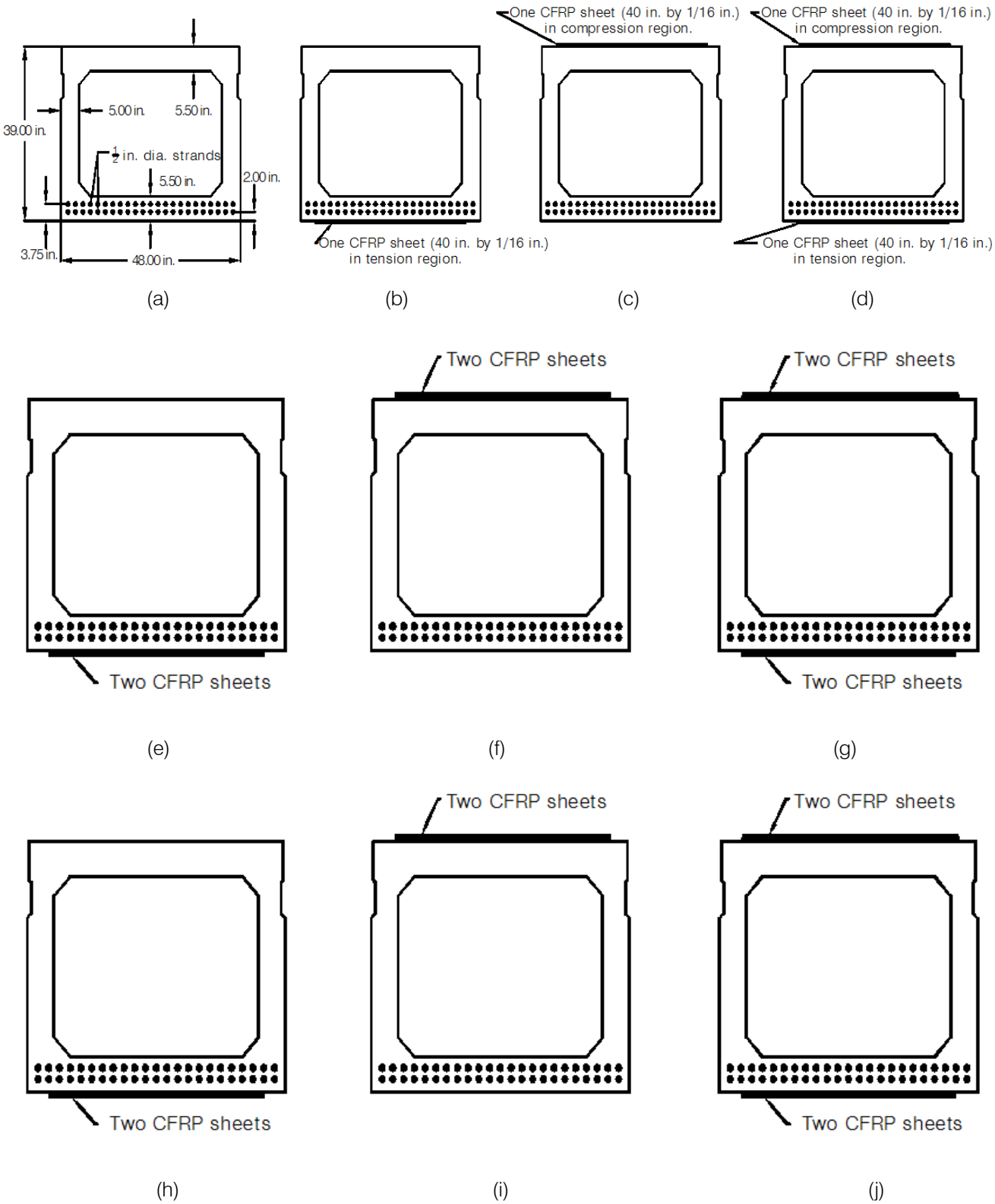

Figure 2: Non-retrofitted box beam section (a), and CFRP retrofitted box beam sections (b) through (j)

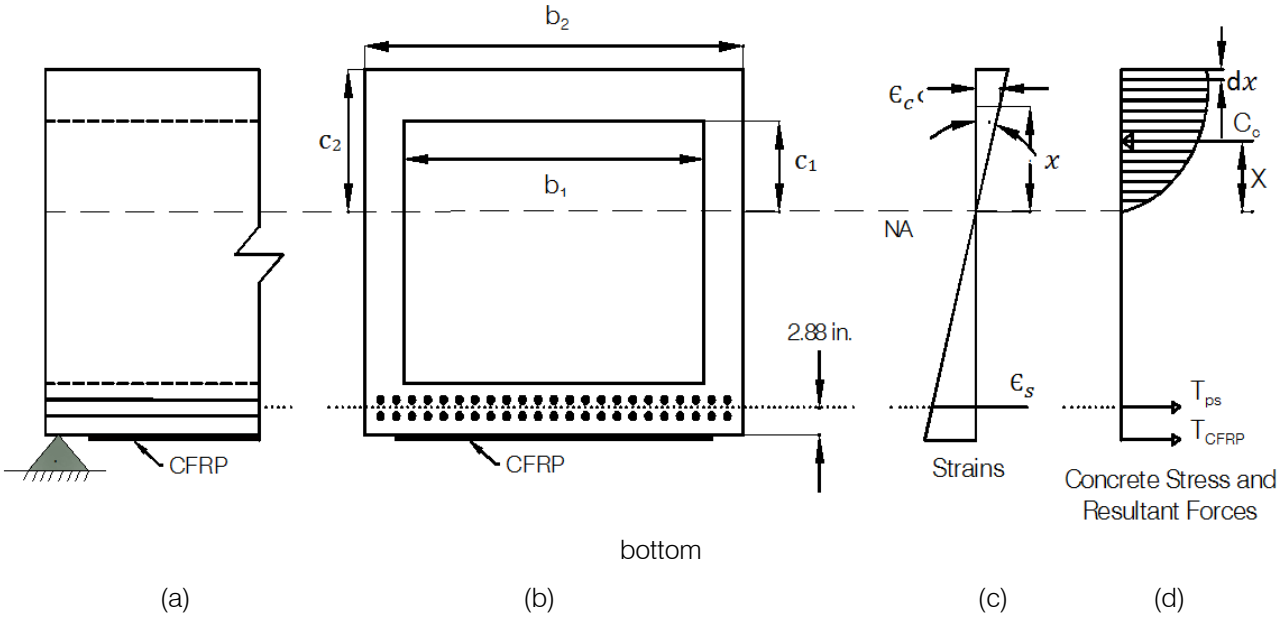

Figure 3: Strain and stress distribution for a simply-supported concrete box beam with CFRP retrofitting at the

Moment-curvature relations are developed for seven different loading stages, namely, at zero external moment, zero strain in concrete at the c.g. of the strands, cracking moment, concrete strain reaching 0.001, 0.002, 0.00248, and 0.003 in./in. The linear portion of the moment-curvature relation is developed using elastic stress-strain distribution. The nonlinear portion of the M-ϕ relation is developed by first assuming the top concrete strain and then determining the NA location iteratively until the axial force equilibrium is satisfied. The converged moment and curvature values are then found using the resulting forces and strain distribution. Using this procedure, the M-ϕ curves are developed for the retrofitted cross sections shown in Figures 2b-2d, 2e-2g, and 2h-2j, respectively. These curves are presented in Figures 4, 5, and 6 including the curve for the non-retrofitted section shown in Figure 2a.

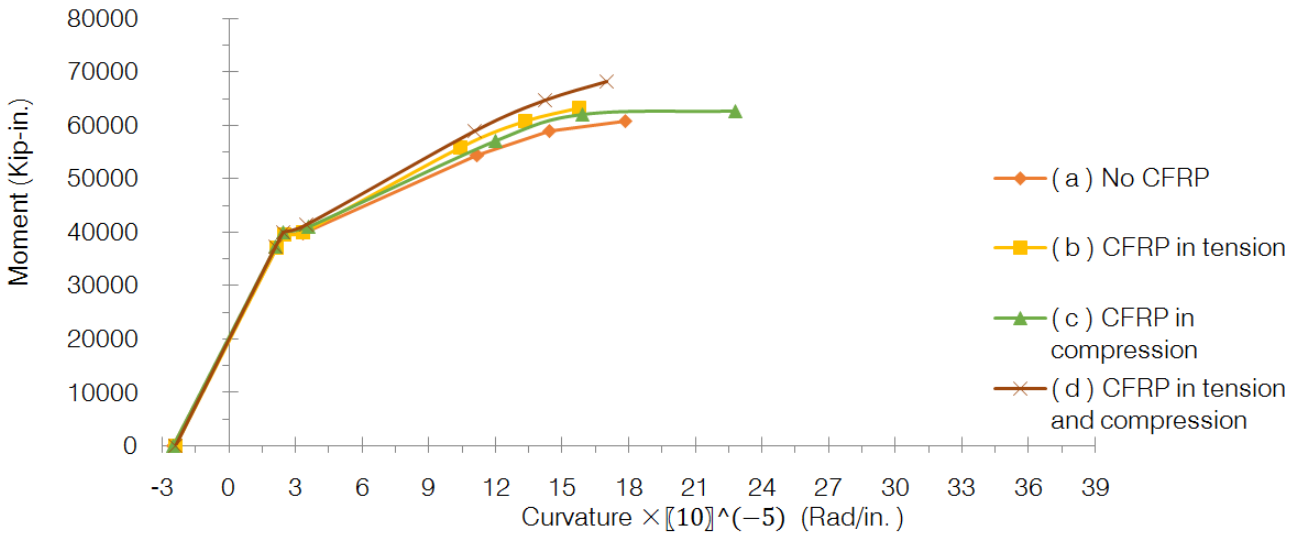

Figure 4: Moment-curvature curves for sections in Figures 2a-2d

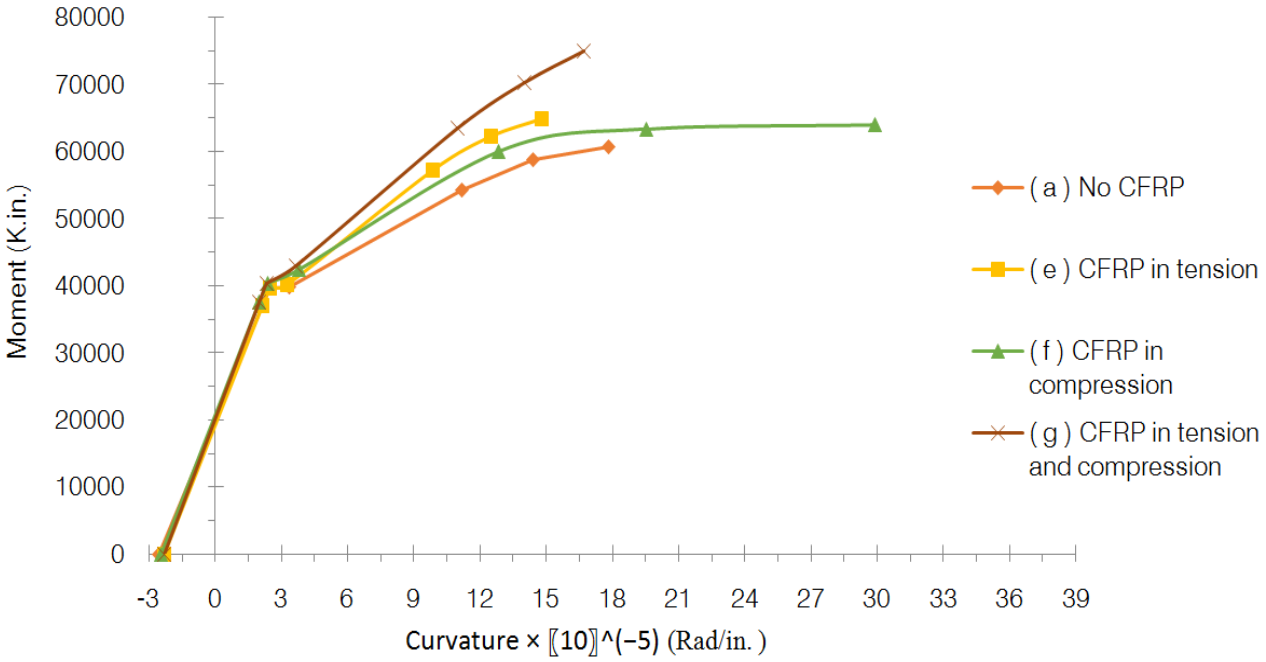

Figure 5: Moment-curvature curves for sections in Figures 2a and 2e-2g

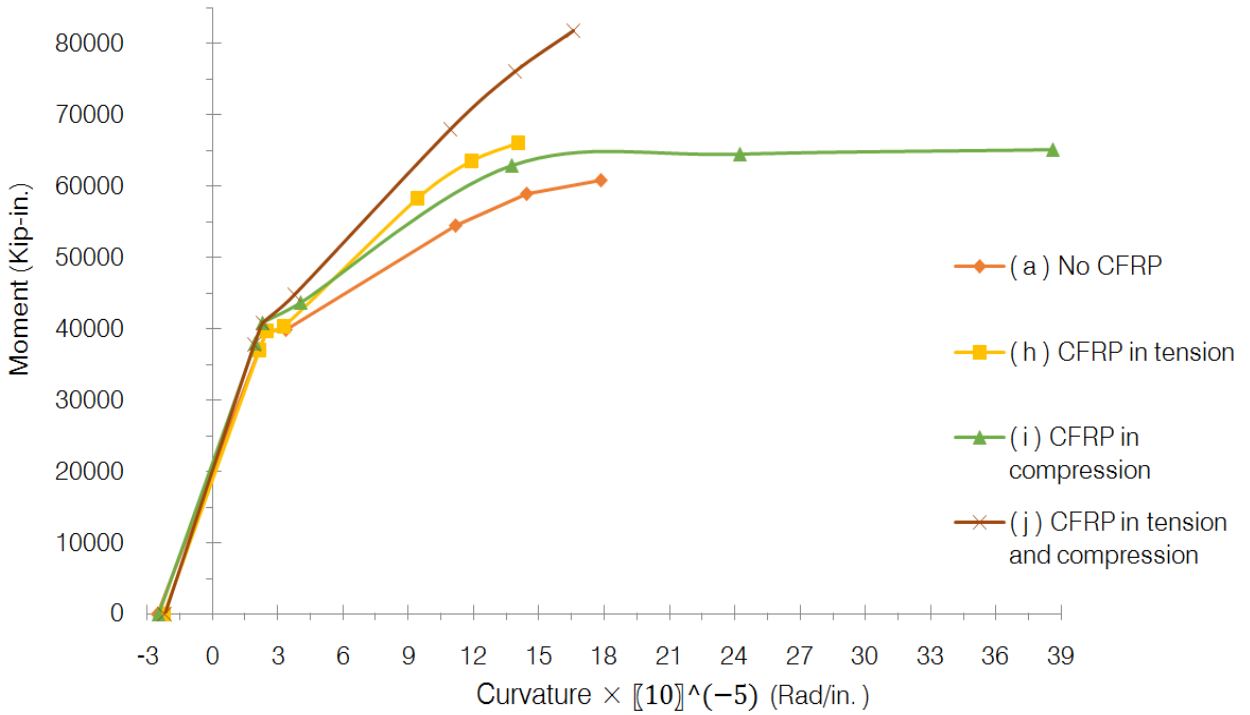

Figure 6: Moment-curvature curves for sections in Figures 2a and 2h-2j

The approximate equation for the linear portion of the M-ϕ relations shown in Figures 4-6 is:

$$\phi = (0.00012M - 2.4) \times 10^{-5} \quad (8)$$

For the nonlinear portion of the M-ϕ relations corresponding to the sections shown in Figures 2a through 2j, the M-ϕ relations are as follow:

$$\phi_a = (0.14 \times e^{0.00008M}) \times 10^{-5} \quad (9)$$

$$\phi_b = (0.195 \times e^{0.00007M}) \times 10^{-5} \quad (10)$$

$$\phi_c = (0.136 \times e^{0.00008M}) \times 10^{-5} \quad (11)$$

$$\phi_d = \phi_e = (0.3 \times e^{0.00006M}) \times 10^{-5} \quad (12)$$

$$\phi_f = (0.12 \times e^{0.00008M}) \times 10^{-5} \quad (13)$$

$$\phi_g = (0.0004M - 13.7) \times 10^{-5} \quad (14)$$

$$\phi_h = M^{2.935} \times 10^{-18} \quad (15)$$

$$\phi_i = (0.035 \times e^{0.0001M}) \times 10^{-5} \quad (16)$$

$$\phi_j = (0.0003M - 9.5) \times 10^{-5} \quad (17)$$

Equations 9 through 17 are obtained using Excel curve-fitting for use in load-deflection analysis based on finite-difference procedure. It is noteworthy that the same moment-curvature given by Equation 12 is found to be applicable to both of the box sections in Figures 2d and 2e. Also, in developing Equations 11, 13, and 16, the last point shown on the curves in Figures 4, 5, and 6 for sections 2c, 2f, and 2i, respectively, are excluded. However, these last points were included separately in the solution algorithm.

IV. Solution Algorithm

To predict the load-deflection relations for the prestressed box beam both without and with CFRP retrofitting, an algorithm is formulated based on the nonlinear moment curvature relations coupled with a finite-difference procedure. Figure 7 shows the finite-difference discretization along the longitudinal z axis of the box beam. The node numbers i = 1, 2, …, N used in the finite-deference formulation are also shown in this figure, with nodes 0 and N+1 as the so-called phantom points. In this study, the segment length h is taken as L/10, where L is the total span of 95 ft. The curvature ϕ_i of the box beam at any node i can be expressed in the following central finite-deference form [15]:

$$\phi_i = \left(\frac{d^2v}{dz^2}\right)_i = \frac{V_{i-1} - 2V_i + V_{i+1}}{h^2} \quad (18)$$

In this equation, V_i is the deflection at any node i. Applying Equation 18 at i = 1, 2, …, N, the following matrix expression is obtained:

$$[\,Q\,] \times \{\,V\,\} = h^2\,\{\,\phi\,\} \quad (19)$$

where [Q] is a N×N coefficient matrix, and {V} is a deflection vector defined by:

$$\{\,V\,\}^T = \{\,V_0, V_2, V_3, \ldots, V_{N-1}, V_{N+1}\,\} \quad (20)$$

The curvature vector is defined by:

$$\{\ \phi\ \}^T = \{\,\phi_1, \phi_2, \phi_3, \ldots, \phi_N\} \quad (21)$$

In Equation 19, the following zero deflection boundary conditions are incorporated: $V_1 = 0$, $V_N = 0$

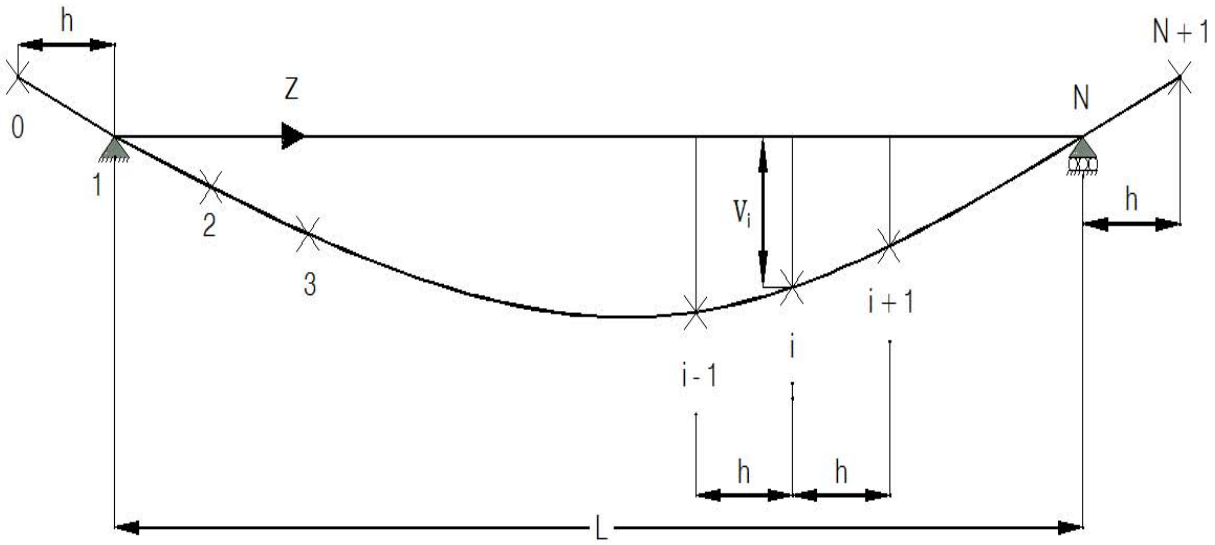

Figure 7: Finite-difference discretization

For a given load level, bending moment value at any location z along the length of the beam is found using the following expressions in their applicable ranges:

$$M_I = (4.721P \times z) + (570w \times z) - (w \times z^2/2) \text{ for } 0 \le z \le 430 \text{ in.} \quad (22a)$$

$$M_{II} = 1720P + (0.721P \times z) + (570w \times z) - (w \times z^2/2) \text{ for } 430 \text{ in.} \le z \le 598 \text{ in.} \quad (22b)$$

$$M_{III} = 4112P - (3.279P \times z) + (570w \times z) - (w \times z^2/2) \text{ for } 598 \text{ in.} \le z \le 766 \text{ in.} \quad (22c)$$

$$M_{IV} = 4878P - (4.279P \times z) + (570w \times z) - (w \times z^2/2) \text{ for } 766 \text{ in.} \le z \le 1140 \text{ in} \quad (22d)$$

In order to develop a load-deflection relation, the following algorithm is formulated and programmed:

1. Define the box beam length, cross-sectional and material properties, intensity of the distributed load w, and a value of P.
2. Discretize the box beam into (N-1) equidistant panels each of length h, associated with cross-sectional nodes i = 1, 2, 3, …, N.
3. Calculate the values of the bending moment M using Equations 22a-22d as applicable for nodes i = 1, 2, 3, …, N.
4. Using the bending moment values from step 3, calculate the curvature ϕ values for the same nodes using Equations 9-17 as applicable, and form the vector of curvatures, { ϕ }.
5. Substitute { ϕ } into Equation 19 and solve for the deflection vector { V }.

Based on the values found in { V }, the largest deflection is found to be at node 6 when N = 11 is used in the present study. Using this procedure, the load-deflection curves for the retrofitted cross sections shown in Figures 2b-2d, 2e-2g, and 2h-2j are developed and shown in Figures 8-10 including the curve for the non-retrofitted section shown in Figure 2a.

V. Results

Table 1 presents a summary of the results based on a rigorous nonlinear analysis of the box beam shown in Figure 1. In this table, c_2 represents the location of the neutral axis at collapse. The values of the collapse load and the corresponding maximum bending moment are represented by P_{max} and M_{max}, respectively. When nondimensionalized using P_{max} and M_{max} values for the non-retrofitted box beam section 2a, they are entered as p_{max} and m_{max} values in this table. It is seen that the p_{max} values for various retrofitting schemes range from 1.05 to 1.52 showing that the retrofitting scheme using section 2j is the most effective of the ones investigated in this study. The range of m_{max} values is seen to be from 1.03 to 1.35. The second most effective retrofitting scheme corresponds to the section 2g providing a p_{max} value of 1.35.

Figure 11 shows the relationships between box beam moment capacity and the CFRP thickness. The upper curve is for retrofitting with CFRP in both tension and compression, and the lower curve is when CFRP is used only in tension. A comparison of the two curves in this figure shows clearly that CFRP retrofitting is significantly more effective when used in both tension and compression regions.

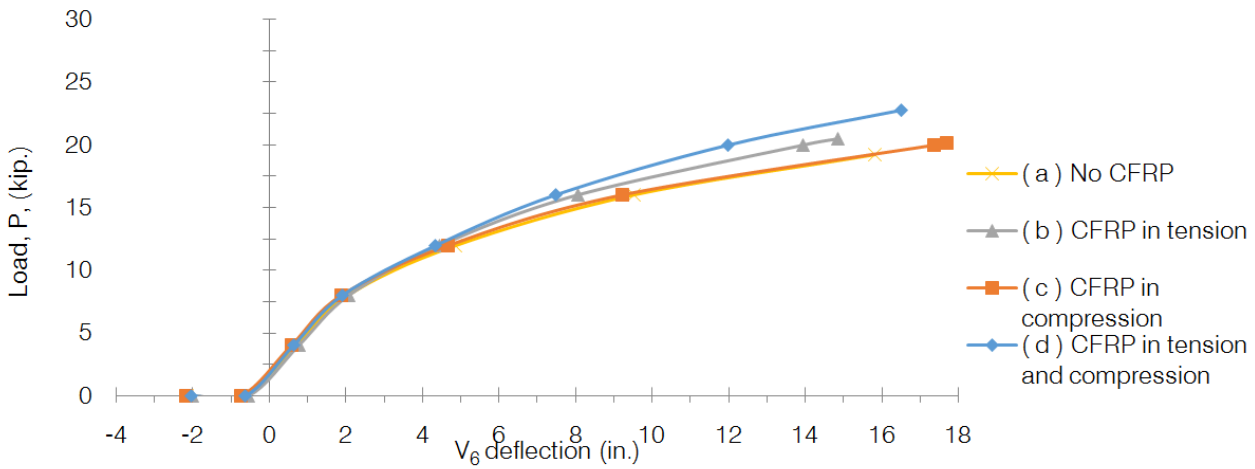

Figure 8: Load-deflection curves for sections in Figures 1a-1d

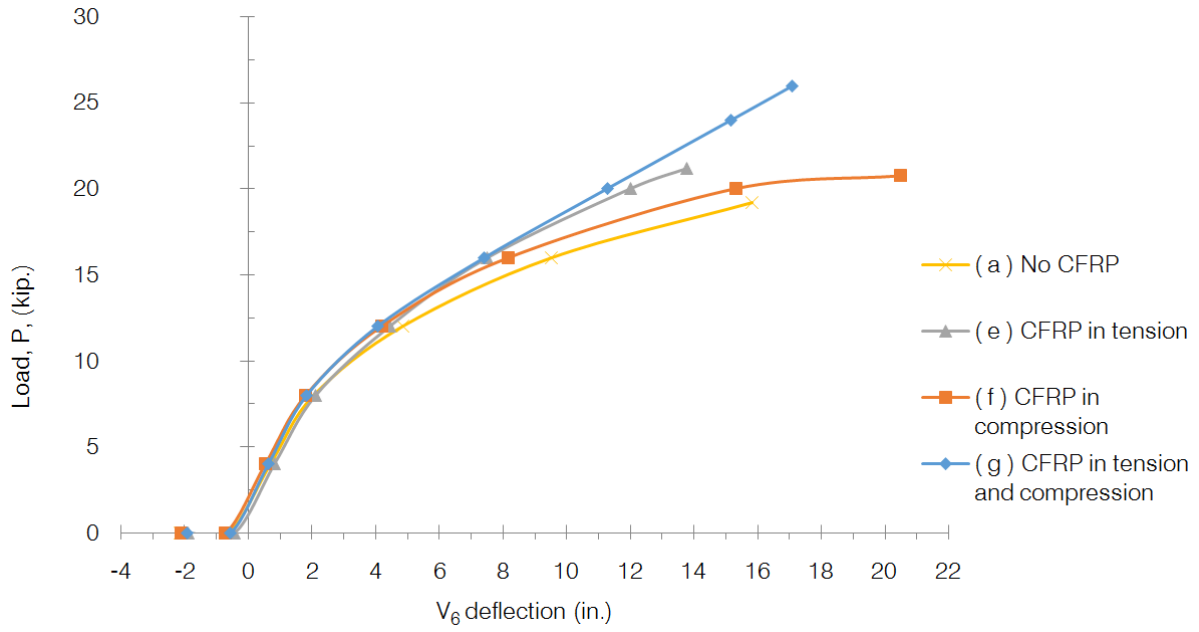

Figure 9: Load-deflection curves for sections in Figures 1a and 1e-1g

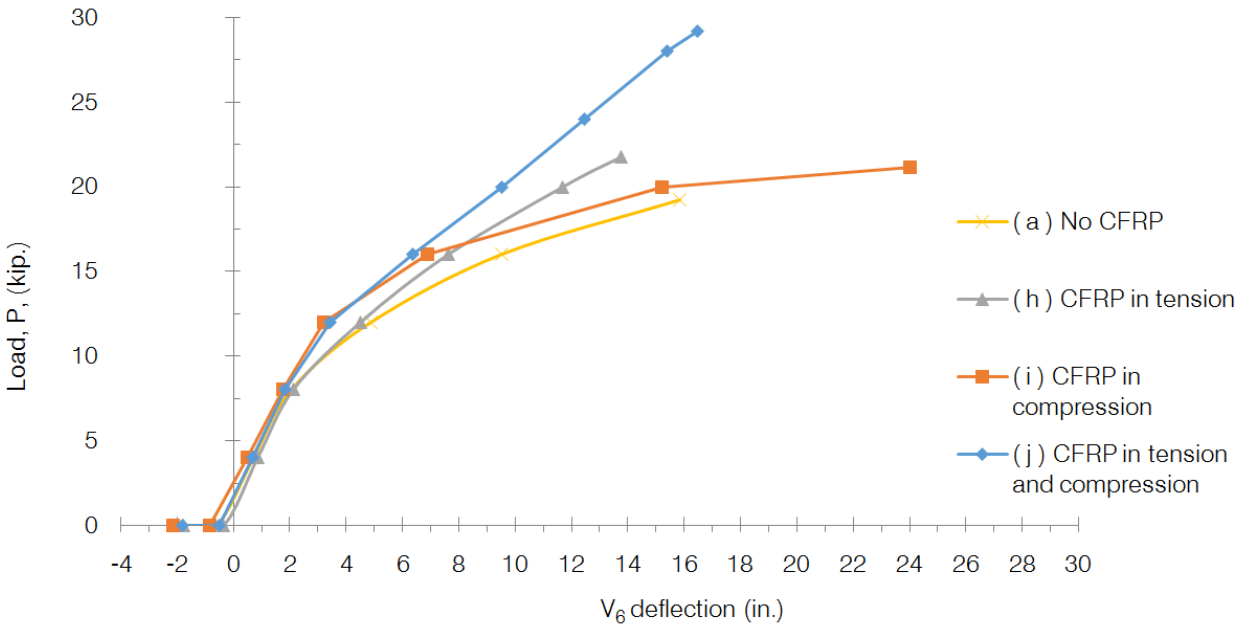

Figure 10: Load-deflection curves for sections in Figures 1a and 1h-1j

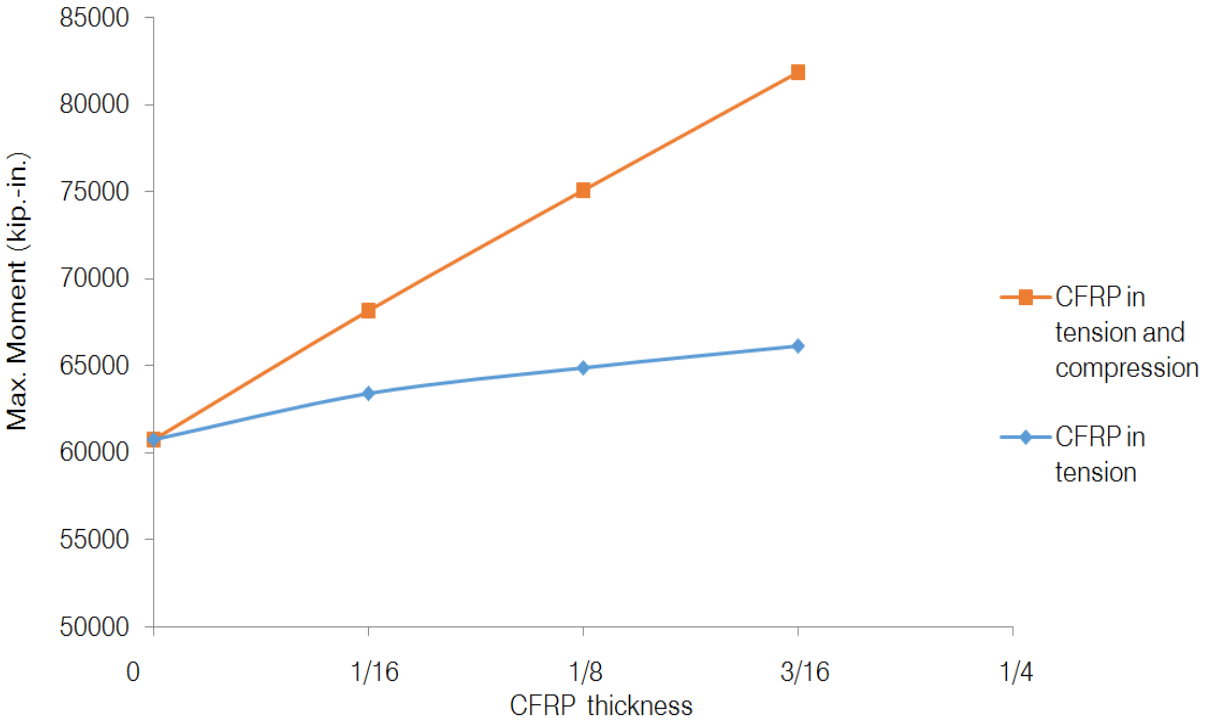

Figure 11: Box beam moment capacity versus CFRP thickness

Table 1: Summary of box beam results at P_{max}

Section (Figure 2)	c_2 (in.)	P_{max} (kips)	p_{max}	M_{max} (kip-in.)	m_{max}
2a	16.81	19.22	1.00	60749	1.00
2b	19.02	20.45	1.06	63364	1.04
2c	13.16	20.12	1.05	62657	1.03
2d	17.64	22.73	1.18	68175	1.12
2e	20.3	21.17	1.10	64876	1.07
2f	10.04	20.78	1.08	64058	1.05
2g	17.94	25.98	1.35	75069	1.23
2h	21.38	21.74	1.13	66098	1.09
2i	7.77	21.27	1.11	65088	1.07
2j	18.12	29.19	1.52	81852	1.45

VI. Conclusions

The following conclusions are drawn from this study:

1. The use of a 3/16-inch thick CFRP retrofitting layer in both tension and compression regions resulted in the largest increase in the load carrying capacity of the box beam.
2. Retrofitting with CFRP simultaneously in both tension and compression regions is for more effective than retrofitting in just the tensile or the compressive region of the box beam.
3. Retrofitting with CFRP in tension only results in practically the same load carrying capacity of the box beam as that obtained with CFRP in compression only.

The nonlinear analysis procedure presented is found to give rapid convergence for the box beam problem studied.

References Références Referencias

1. O. Rosenboom and S. Rizkalla. Behavior of Prestressed Concrete Strengthened with Various CFRP Systems Subjected to Fatigue Loading. ASCE: Journal of Composites for Construction, No. 10(6), 2006, pp. 492-502.

2. S. Petro. Series of bridges in phoenix strengthened successfully. http://www.gannettfleming.com. Accessed April 10, 2014.
3. P. Rusinowski and B. Täljsten. Intermediate Crack Induced Debonding in Concrete Beams Strengthened with CFRP Plates. Advances in Structural Engineering, No. 12(6), 2009, pp. 793-806.
4. Burningham, C. A., Pantelides, C. P., and L.D. Reaveley. Repair of Prestressed Concrete Beams with Damaged Steel Tendons Using Post-Tensioned Carbon Fiber-Reinforced Polymer Rods. ACI Structural Journal, No. 111(2), 2014, pp. 387-395.
5. Y. J. Kim, M. F. Green, and R. Wight. Flexural behavior of reinforced or prestressed concrete beams including strengthening with prestressed carbon fiber reinforced polymer sheets. Canadian Journal of Civil Engineering, No. 34(5), 2007, pp. 664-677.
6. Y. J. Kim, S. Chen, and M. F. Green. Ductility and Cracking Behavior of Prestressed Concrete Beams Strengthened with Prestressed CFRP Sheets. Journal of Composites for Construction, No. 12(3), 2008, pp. 274-283.
7. N. Grace, E. Jensen, V. Matsagar, and P. Penjendra. Performance of an AASHTO Beam Bridge Prestressed with CFRP Tendons". Journal of Bridge Engineering, No. 18(2), 2013, pp. 110-121.
8. A. Bennitz, J. Schmidt, J. Nilimaa, B. Täljsten, P. Goltermann, and D. Ravn. Reinforced Concrete T-Beams Externally Prestressed with Unbonded Carbon Fiber-Reinforced Polymer Tendons. ACI Structural Journal, No. 109(4), 2012, pp. 521-530.
9. M. Aram, C. Czaderski, and M. Motavalli, M. Effects of Gradually Anchored Prestressed CFRP Strips Bonded on Prestressed Concrete Beams. ASCE: Journal of Composites for Construction, No. 12(1), 2008, pp. 25-34.
10. C. E. Reed and R. J. Peterman. Evaluation of Prestressed Concrete Girders Strengthened with Carbon fiber reinforced polymer Sheets. Journal of Bridge Engineering, No. 9(2), 2004, pp. 185-192.
11. P. A. Ritchie, D. A. Thomas, L. W. Lu, and G. M. Connelly. External reinforcement of concrete beams using fiber reinforced plastics. ACI Structural Journal, No. 88(4), 1991, pp. 490-500.
12. N. Chagnon and B. Massicotte. Seismic retrofitting of rectangular bridge piers with CFRP". Canada, 2005, pp. 1-10.
13. AASHTO. LRFD Bridge Design Specifications. American Association of State Highway and Transportation Officials, Loose Leaf, 2014.
14. T. Y. Lin, and N. H. Burns. Design of prestressed concrete structures. John Wiley & Sons, Incorporated, New Jersy, 1981.
15. A. R. Mitchell and D. F. Griffiths. The finite difference method in partial differential equations. Wiley, New York, 1980.